Geophysical Research Letters

RESEARCH LETTER
10.1029/2018GL078566

Key Points:
- Intense plasma waves are observed simultaneously with broad energy spectrum of precipitating electrons
- The waves are propagating in the whistler mode in the same direction as the electrons
- The intense whistler mode waves are not observed during nearby inverted V events

Supporting Information:
- Supporting Information S1

Correspondence to:
W. S. Kurth,
william-kurth@uiowa.edu

Citation:
Kurth, W. S., Mauk, B. H., Elliott, S. S., Gurnett, D. A., Hospodarsky, G. B., Santolik, O., et al. (2018). Whistler mode waves associated with broadband auroral electron precipitation at Jupiter. *Geophysical Research Letters*, *45*, 9372–9379. https://doi.org/10.1029/2018GL078566

Received 28 APR 2018
Accepted 28 AUG 2018
Accepted article online 4 SEP 2018
Published online 23 SEP 2018

Whistler Mode Waves Associated With Broadband Auroral Electron Precipitation at Jupiter

W. S. Kurth[1], B. H. Mauk[2], S. S. Elliott[1], D. A. Gurnett[1], G. B. Hospodarsky[1], O. Santolik[3,4], J. E. P. Connerney[5,6], P. Valek[7], F. Allegrini[7,8], G. R. Gladstone[7,8], S. J. Bolton[7], and S. M. Levin[9]

[1]Department of Physics and Astronomy, The University of Iowa, Iowa City, IA, USA, [2]The Johns Hopkins University Applied Physics Laboratory, Laurel, MD, USA, [3]Department of Space Physics, Institute of Atmospheric Physics, The Czech Academy of Sciences, Prague, Czechia, [4]Faculty of Mathematics and Physics, Charles University, Prague, Czechia, [5]Space Research Corporation, Annapolis, MD, USA, [6]Goddard Space Flight Center, Greenbelt, MD, USA, [7]Southwest Research Institute, San Antonio, TX, USA, [8]University of Texas at San Antonio, San Antonio, TX, USA, [9]Jet Propulsion Laboratory, Pasadena, CA, USA

Abstract Large amplitude electromagnetic plasma waves are observed simultaneously with intense fluxes of electrons precipitating on auroral field lines at Jupiter. Here we present plasma wave observations from the Juno Waves instrument obtained during an instance of very intense broadband electron precipitation observed by the Jupiter Energetic Particle Detector Instrument connecting to Jupiter's main auroral oval. The wave spectrum extends from 50 Hz to ~10 kHz with peak-to-peak amplitudes of ~10 nT in the magnetic channel and of ~1 V/m in the electric channel, representing some of the most intense plasma waves observed by Juno. The *E* and *B* fields of these electromagnetic waves are correlated and have apparent polarization perpendicular to Jupiter's magnetic field with a downward Poynting flux. We conclude the plasma waves are whistler mode emissions with a possible admixture of ion-cyclotron or Alfvén waves and may be important in the broadband electron acceleration.

Plain Language Summary Large amplitude whistler mode waves are found coincidently with intense fluxes of precipitating electrons across a broad energy range connecting to Jupiter's main auroral oval. The whistler mode waves are propagating downward, in the same direction as the precipitating electrons. The tight correspondence in time between the waves and the electrons strongly suggests an important interaction between the waves and electrons.

1. Introduction

Mauk, Haggerty, Paranicas, et al. (2017b) and Mauk et al. (2018) showed that energetic electrons precipitating into Jupiter's main auroral oval can take the form of a classic "inverted V" spectrum or a broadband spectrum. The inverted V implies that a field-aligned potential is responsible for the acceleration of the electrons. The broadband energetic electron spectrum requires a stochastic acceleration process. These authors show evidence that what starts out as an inverted V spectrum transforms into a broadband spectrum, possibly because of an instability that sets in at some threshold in the field-aligned potential (Mauk et al., 2018). Here we show evidence of very intense electromagnetic plasma waves found simultaneously with the broadband electron spectrum, strongly suggesting that the plasma waves are in some way tied to the stochastic acceleration.

Juno's polar orbit at Jupiter provides an excellent opportunity to explore the physics of Jupiter's auroras (Bolton et al., 2017). The mission includes a payload designed to provide measurements of energetic particles, fields, and remote sensing observations as the spacecraft traverses magnetic field lines threading the planet's auroral features. In this paper we concentrate on one such passage over the main auroral oval at a radial distance of 1.64 Jovian radii (R_J) obtained during Juno's perijove (PJ) 7 on 11 July (day 192) 2017.We primarily report plasma wave observations by the Juno Waves instrument (Kurth et al., 2017) organized by Juno's magnetic field measurements (Connerney et al., 2017) and compared with Mauk et al. (2018) observations by the Jupiter Energetic Particle Detector Instrument (JEDI) described by Mauk, Haggerty, Jaskulek, et al. (2017a).

For this paper, we will rely heavily on Waves observations utilizing both its electric dipole antenna and search coil magnetometer. The electric (E_y) antenna has an effective axis that is parallel to the spacecraft *y* axis;

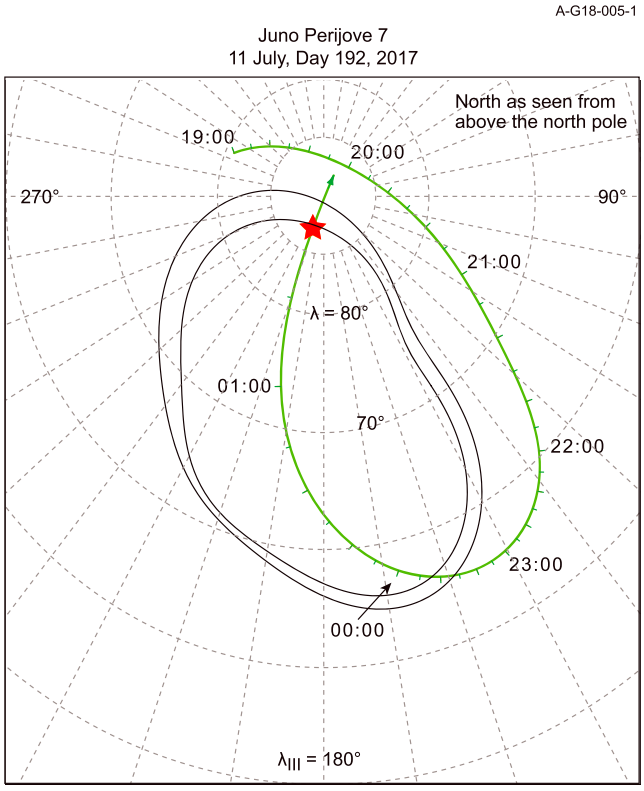

Figure 1. Position of Juno mapped to the 1-bar level using the JRM09 magnetic field model (Connerney et al., 2018). The two solid lines show the statistical location of Jupiter's north auroral oval (Bonfond et al., 2012).

hence, it rotates with the spacecraft that spins about its *z* axis. The geometric effective length is 2.41 m used in the field strengths given herein, but see Kurth et al. (2017) electrical considerations that may yield a shorter effective antenna. The search coil is aligned with the spin axis. Hence, the magnetic component detected (B_z) is in a direction orthogonal to the electric antenna and is not spin modulated. For times near PJ, particularly early in the mission, the angle between the search coil and Jupiter's magnetic field is close to 90°.The Waves instrument has a pair of channels in its low-frequency receiver (LFR) that extend from 50 Hz to 20 kHz allowing for simultaneous measurements by both sensors. The LFR captures waveforms with 16-bit analog-to-digital converters sampling at a rate of 50 ksps. For modes used in this paper, the two channels are sampled simultaneously, allowing comparisons of the phase of the two channels. One difference between the electric and magnetic channels is that the electric channel utilizes automatic gain adjustments to allow for a larger dynamic range than afforded by the 16-bit analog-to-digital converter. The magnetic channel has no such variable gain amplifier. For survey measurements, the onboard digital signal processor performs fast Fourier transforms of the waveform measurements and constructs a quasi-logarithmic spectrum by binning Fourier components. For burst mode measurements, the actual waveforms can be stored and later telemetered to the ground for full resolution analyses. The LFR waveforms are collected once per second in series comprising 6,144 contiguous samples covering 123 ms.

2. Observations

The observations in this paper were obtained on field lines threading the statistical auroral oval determined from HST images (Bonfond et al., 2012). We use the JRM09 magnetic field model (Connerney et al., 2018) to map Juno's position to the planet. Mauk et al. (2018) showed the projection of Juno's position onto Juno ultraviolet images of the auroral oval in their Figure 2b.We focus on observations on 11 July, day 192, 2017 between 01:14:15 and 01:16:15 UT. Figure 1 shows this location marked in red. Figure 2 presents the energetic electron and associated plasma wave observations covering time intervals represented in Figures 3 and 4 of Mauk et al. (2018). In the right-hand column of Figure 2h we repeat the observations in Figure 4c of Mauk et al. (2018) that show the energy spectra for downward-going electrons. In panels i and j we show burst mode electric and magnetic spectrograms, respectively, showing the spectral density as a function of frequency and time. The spectra for both the electric and magnetic fields (shown in Figures 3a and 3b) are at their maxima near 50 Hz, the lowest frequency measured, and show a small notch at the proton cyclotron frequency f_{cp}. The electric spectrum shows a cutoff at about 10 kHz, possibly at the electron plasma frequency f_{pe}, above which the whistler mode cannot propagate and consistent with the electron density from the plasma instrument at this time. Figures S1 and S2 in the supporting information give individual electric and magnetic spectra for 15 waveform captures, respectively, during the interval including the inverted V and broadband electron precipitation event. In the presence of the intense Jovian magnetic field, the fluxgate magnetometer does not detect lower frequency waves associated with this event. Figure 2k presents an assessment of the ratio E/cB for the waves. The values plotted for this ratio during the intense wave feature and surrounding wave features are close to 1, indicating an electromagnetic wave. The ratio is computed from survey data which are spectral densities computed onboard and binned into log-spaced frequency channels. We also note that spin modulation nulls are visible in the electric channel due to the electric antenna being oriented perpendicular to the spacecraft spin axis. Hence, the ratio will be underestimated during these nulls.

Mauk et al. (2018) pointed out that the inverted V feature between 01:15:45 and 01:15:55 is likely due to a field-aligned potential. The plasma instrument sees this move into its energy range shortly after 01:15:55. During the inverted V event, Mauk et al. also report upward going protons, consistent with the same field-aligned potential. However, between about 01:15:50 and 01:15:53, the peaked feature in the electron

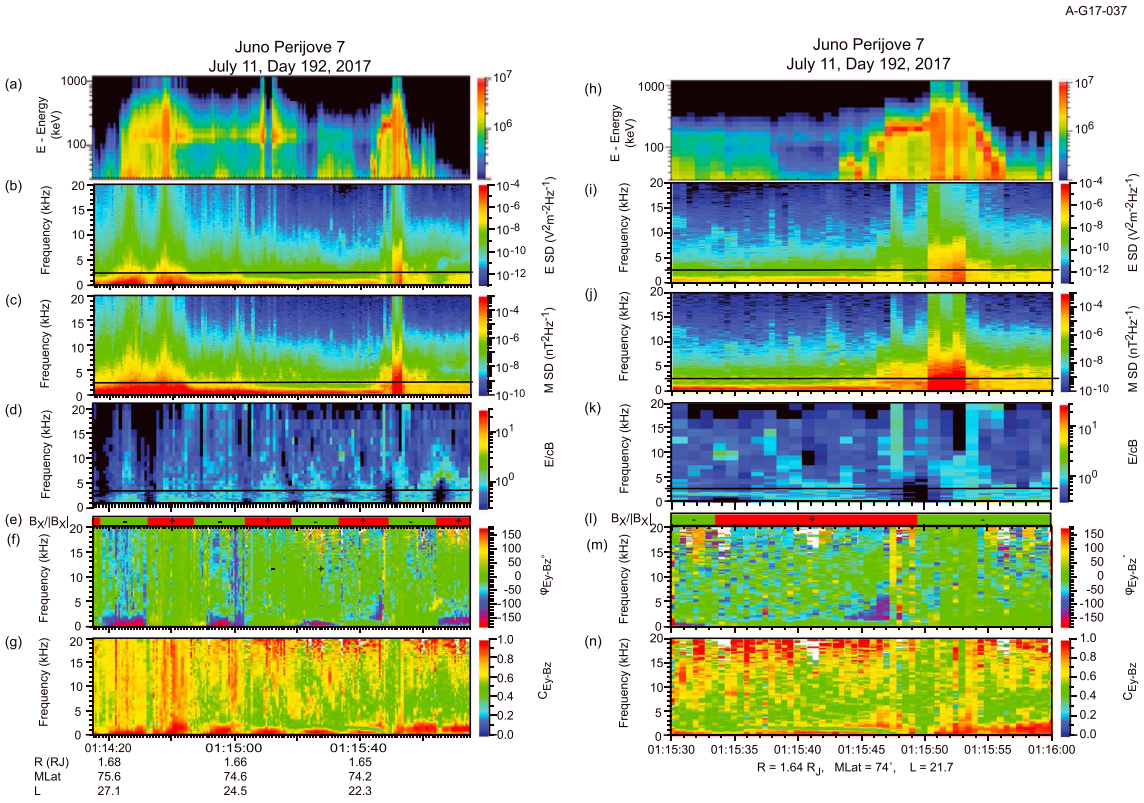

Figure 2. Observations of downward-going energetic electrons and associated plasma waves. (a) Downward-going electrons with energies up to 1 MeV. b) Electric field spectrogram for the frequency range 50 Hz to 20 kHz. The black line is f_{cp}. (c) Magnetic field spectrogram for the same frequency range as panel b. (d) Calculation of the ratio E/cB for the waves. (e) The sign of the planetary B_x magnetic field component. (f) The phase between the signals detected by the electric and magnetic sensors. This phase, along with the sign of the x component of Jupiter's magnetic field in spacecraft coordinates, gives the direction of propagation parallel or antiparallel to Jupiter's field. (g) Coherence between the E_y and B_z components of the waves in panels b and c.(h–n) Formatted the same as in the left column, but focusing on the event at 01:15:52.

spectrum is replaced by a broadband energy spectrum up to ~1 MeV accounting for an energy flux of ~3,000 mW/m^2. The plasma instrument observes primarily downgoing electrons greater than a few keV at the same time. Simultaneously, the upward going protons disappear. It is precisely at this time that the Waves data show a very strong electromagnetic emission. The striking simultaneity of this burst of wave activity with the breakdown of the field line potential into a stochastic process is what drew our attention. As will be shown below, the magnetic components of these waves are some of the strongest observed during the Juno mission and saturate the sensor and/or receiver. In section 3 we will consider the propagation mode of these waves.

The left column in Figure 2 shows the JEDI and Waves data in a similar format as for right hand column, but for a somewhat longer time interval. A similar broadband energy spectrum of bidirectional electrons is centered near 01:14:38. Interestingly, this event was accompanied by a downward going proton inverted V with the beam spreading toward perpendicular. Mauk et al. (2018) interpret this as evidence for a downward directed, field-aligned electric field at significant distances above the planet; the broadening of the beam is likely due to mirror forces and possibly wave scattering. The broadband precipitating electron event is, again, accompanied by intense, broadband electromagnetic plasma waves.

3. Assessment of Wave Mode

In this section we examine the plasma waves observed between 01:15:50 and 01:15:53 UT to determine their mode of propagation. Figure 2k shows the wave E/cB as a function of frequency and time. The values shown range from much less than 1 to about 1. The electric field is spin modulated. Just prior to 01:15:50 the dipole antenna is nearly parallel to Jupiter's magnetic field **B**. Hence, for a wave polarized perpendicular to **B**, the electric field is underestimated when the antenna is near parallel to **B**. And, given that the magnetic signal

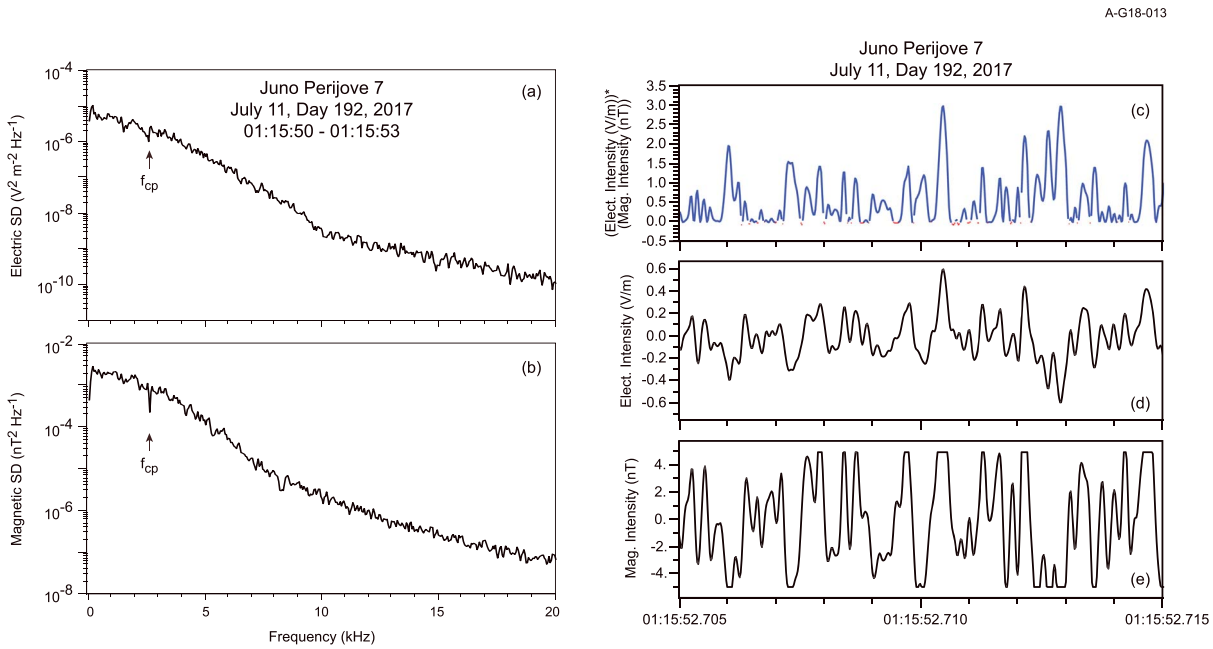

Figure 3. (a) Electric field spectrum averaged over three 123-ms waveform captures. (b) Magnetic field spectrum averaged over three 123-ms waveform captures from the same times as those in panel a. Note that there is a high-pass filter at 50 Hz for both the electric and magnetic channels. Correlation of electric and magnetic waveforms for a 10-ms interval during the event shown in Figure 2. (c) The result of multiplying simultaneously measured (d and e) *E* and *B* waveform measurements. Note that this simply shows that the *y* component of the electric wave field is either in phase or out of phase with the *z* component of the magnetic wave field and does not, by itself, imply direction of propagation. (d) The electric field waveforms. (e) The magnetic field waveforms; note the clipping at ±5 nT.

is saturated, the ratio may be overestimated. We provide this ratio as evidence of the electromagnetic character of the waves, but the quantity is not known, accurately.

In Figure 2m we plot the phase between the E_y and B_z components of the wave (in payload coordinates) using simultaneous measurements in burst waveforms. During this interval, the search coil is nearly perpendicular to **B** (actually 95.5°) while the electric antenna rotates from near parallel (or antiparallel) to perpendicular to **B** twice per spacecraft spin. This configuration can be used to determine the direction of the Poynting flux as a function of frequency under some circumstances (Mosier & Gurnett, 1971). Such an analysis was used by Kolmasova et al. (2018) to determine the direction of propagation of lightning whistlers using Juno observations. During the event near 01:15:52, Figure 2m indicates that the wave E_y and B_z are in phase. Figure 2n shows a reasonable degree of coherence between the electric and magnetic field waveforms. A greatly expanded view of this phase analysis is given in Figure S3 and shows the details of the phase and coherence at the time of interest. According to Kolmasova et al. (2018), if E_y and B_z are in phase in the northern hemisphere and the *x* component of **B** is positive, then the waves are propagating in the direction of **B**, hence upgoing (away from Jupiter). However, Figure 2l shows that $B_x/|B_x|$ is negative, so we conclude the waves in the intense event near 01:15:52 are downgoing. This is the basis for determining the direction of propagation as a function of frequency using the two Waves sensors. In comparison, if we examine the data near 01:14:37, the phase is similar to 01:15:52, but B_x is positive; hence, these waves are propagating upward from Jupiter.

Figure 3 allows an alternate examination of the correlation between the electric and magnetic fields for 10 ms beginning at 01:15:52.700 UT. Figures 3d and 3e show the electric and magnetic waveforms, respectively. Note that the peak-to-peak amplitude of the electric field is about 1 V/m while the magnetic field is clipped at a peak-to-peak amplitude of 10 nT. The magnetic channel has a single gain state, and this signal clearly exceeds its dynamic range. Nevertheless, we can still see that there is a reasonable degree of correlation between *E* and *B*; Figure S4 shows a correlation coefficient for the waves obtained at 01:15:52.650 of $R = 0.88$, even with the clipping. Figure 3c shows the result of multiplying each value in the electric waveform by the simultaneously sampled magnetic value. The positive products show that the signals are in phase. At this instant in time, the angle between the antenna effective axis and the

Jovian magnetic field is about 140°. Note that Figure 3c emphasizes the lowest frequencies and simply shows whether the E_y component of the wave is in phase or out of phase with the B_z component of the wave; by itself, this does not give the direction of propagation. Figure S3d provides a detailed view of the coherence in frequency and time and shows that for frequencies below about 5 kHz the coherence is very close to 1.

Figures 4a–4d show the interval 01:14:15 to 01:16:15 in the same format as Figure 3 in order to show the effects of the spinning electric field antenna. In Figure 4 the waveforms are so highly compressed that one can only see the envelope of their amplitudes. It can be seen that the instrument collects one waveform packet from each sensor each second. Early in this interval, there are strong electromagnetic waves that are polarized such that both the electric and magnetic components are perpendicular to Jupiter's magnetic field. Figure 4c shows that the magnetic field component is uniformly large until about 01:14:45 when it decreases. The search coil is about 95° from **B**. The wave electric field clearly shows the effect of spin modulation with nulls every half spin, when the antenna is nearly parallel or antiparallel to **B**, as seen in Figure 4d. Hence, in Figure 4a one can see that the phase between *E* and *B* reverses sign each half spin. Note that the peaks in Figure 4a occur when the E_y antenna is at an angle of 90° with respect to **B**. Using the bar above Figure 4a, one can see that the sign of the product of *E* and *B* changes when the sign of the planetary field B_x component changes. Following the same logic as discussed relative to the phase analysis in Figure 2, one can see all of the waves are upgoing except for the intense whistler mode waves centered near 01:15:52. Now, focusing on the event at 01:15:52 shown in Figures 4e–4h, we see the wave magnetic field amplitude is very large, but that of the electric field is less than in the earlier period. However, the electric field amplitude is increasing as the angle between the E_y antenna and **B** decreases from near 180° toward 90°.The event ends, however, before the more favorable perpendicular orientation is achieved.

For the very intense event near 01:15:52, we conclude the following:

1. These waves are very intense. The magnetic field waveform is clipped at peak-to-peak amplitudes of ~10 nT, and electric fields are ~1 V/m.
2. While peaking at the lowest frequencies, the spectrum extends well above the proton cyclotron frequency and shows a cutoff in the electric spectrum that is likely at f_{pe}; hence, this would suggest whistler mode emissions for the higher frequency waves. The cutoff at f_{pe} is not seen in the magnetic spectrum probably due to the clipping, but such is seen at other nearby times as shown in Figure S2. At other times, a strong intensification in the spectrum below f_{cp} can be found, suggestive of ion cyclotron waves.
3. The waves are clearly electromagnetic with *E*/*cB* tending near 1. This ratio is affected by both the variable angle of the electric antenna with Jupiter's magnetic field and the clipped magnetic field signal, hence is not well determined but is sufficiently small to exclude a quasi-electrostatic mode.
4. The phase measurements in Figures 2–4 and S3 and S4 all show that *E* and *B* are correlated in phase, again consistent with an electromagnetic whistler mode emission.
5. Even though the full polarization cannot be determined with the limited number of sensors of the Waves instrument, observations in Figure 4 strongly imply that both *E* and *B* are polarized perpendicular to the magnetic field.
6. The analysis of the Poynting flux direction in Figures 2 and S3 indicates the waves are propagating downward, toward Jupiter.

Therefore, we conclude that the strong broadband plasma waves occurring simultaneously with the strong downgoing broadband electron spectrum observed by JEDI are downgoing whistler mode emissions. Given the strong spectrum below f_{cp}, it is not possible to rule out some admixture of Alfvén waves or ion cyclotron waves at lower frequencies.

Applying a similar analysis to the broadband electron precipitation event at 01:14:38 (see Figure S5 for an expanded view), the wave *E*/*cB* ratio is similar and the E_y-B_z phase is near zero for both the whistler mode as well as the lower frequency component. However, the sign of the planetary B_x component is now positive, and we infer that the whistler mode waves are upgoing instead of downgoing. Recall that these electrons are bidirectional. The electric field spectrum at this time (Figure S6) shows a somewhat elevated intensity below f_{cp}, suggesting the possibility that Alfvén and/or ion cyclotron waves (also upgoing) may play a more important role here.

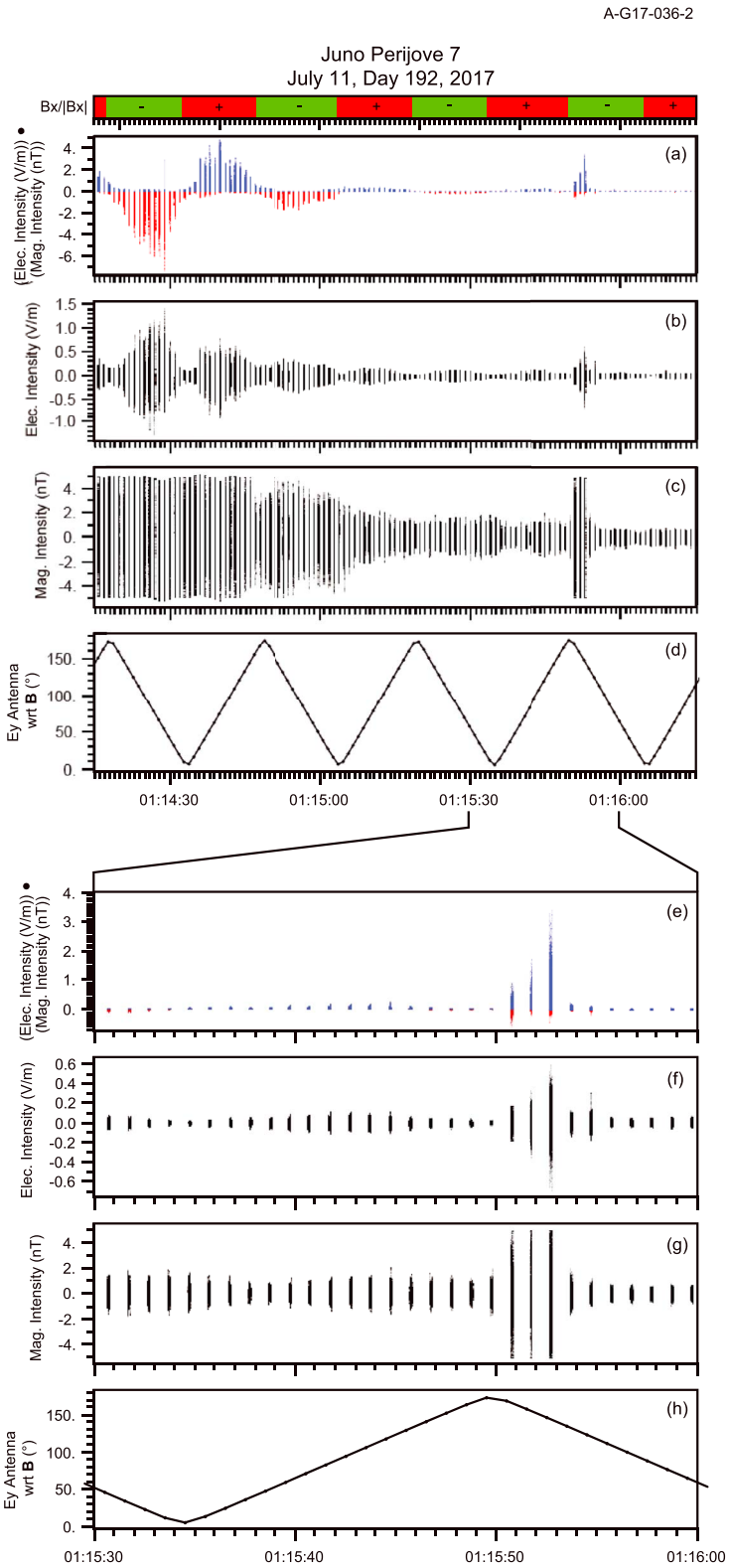

Figure 4. Correlation of electric and magnetic waveforms in a format similar to Figure 3, but with much longer time intervals and with panels d and h that show the angle between the electric antenna and the planetary magnetic field. The bar at the top gives the sign of the B_x component in spacecraft coordinates. Note that the waveform captures are highly compressed in time and simply show amplitude in this presentation. (a–d) The rotation of the electric antenna with respect to Jupiter's magnetic field. (e–h) Interval around the broadband electron precipitation event near 01:15:52, and the electric field is increasing as the angle of the antenna decreases from near parallel toward perpendicular to **B**.

Mauk, Haggerty, Paranicas, et al. (2017b) report an additional broadband electron precipitation event during PJ4 at 13:39:08 on 2 February (day 033) 2017. See Figure S7. Again, a broadband wave spectrum is observed for this event, although the spectrum is sharply peaked below f_{cp}, possibly implying a significant presence of ion cyclotron waves (Figure S8). The spectral peak near 500 Hz, possibly related to helium cyclotron waves, is a factor of 100 stronger than the whistler mode just above f_{cp}. The phase analysis (see Figures S7 and S9) indicates that the whistler mode waves are downgoing but the low frequency waves, below f_{cp}, are upgoing.

4. Discussion and Conclusions

We have shown that very intense whistler mode emissions appear coincidently with some of the strongest precipitating fluxes of electrons observed by Juno (Mauk et al., 2018; Mauk, Haggerty, Jaskulek, et al., 2017a). The wave signature is limited to times when the electron spectrum is broadband as opposed to a peaked inverted V spectrum produced by a field aligned potential. The precise temporal correspondence between the broad-energy precipitation and the strong whistler mode signals lead to the suggestion that the two phenomena are the result of wave-particle interactions, although not necessarily at the current altitude of Juno. There are also strong waves at frequencies below f_{cp}, suggesting that lower-frequency waves such as Alfvén or ion-cyclotron waves may also be important here. Chaston et al. (1999) show broadband Alfvén waves in association with low-energy precipitating electrons in Earth's dayside aurora.

For the intense whistler mode emissions in the three events studied here, there is no evidence of a funnel shape or quasi-electrostatic nature as one would expect for auroral hiss or even VLF saucers with waves propagating on the resonance cone. Rather, these waves appear to be propagating parallel to the magnetic field.

Strangeway et al. (1998) discuss intervals of electron spectra extending over a broad energy range observed at Earth; however, in those cases, the energies are limited to the peak of the inverted V and below. Amm et al. (2002) and Paschmann et al. (2003) point out that auroral hiss found below the electron acceleration region can be driven by the electron beam and is likely responsible for the stabilization of the beam, forming a plateau. Such may be the case in the events studied by Strangeway et al. There are some very important differences between the terrestrial cases and those discussed herein, however. First, the electron precipitation events identified by Mauk et al. (2018) extend to much higher energies than the peak of the nearby inverted V. Second, the VLF waves observed in the terrestrial cases were propagating on the resonance cone, with large E/cB.

While all three examples of broadband electron precipitation discussed by Mauk et al. (2018) exhibit strong whistler mode emissions, each example shows distinctive characteristics. The 01:15:52 event on 11 July shows only a small break in the spectrum below f_{cp}, and the waves and electrons are both downgoing. For the earlier bidirectional electron event near 01:14:38, the whistler mode waves are propagating upward and there is a somewhat stronger spectrum below f_{cp} that is also propagating upward. For the PJ4 event the whistler mode waves are downgoing and waves in the strong peak below f_{cp} are upgoing.

Mauk et al. (2018) show evidence for upward going ions during the inverted V events, similar to what would be expected for the upward current region in Earth's auroral zone (Carlson et al., 1998). There is evidence for a strong peak well below f_{cp} during the inverted V events observed during both PJ4 and PJ7 in the Waves data. These may be electromagnetic ion cyclotron waves that interact with the ions.

We have demonstrated the strong correspondence between probable intense whistler mode waves and intense downward fluxes of electrons with a broad energy spectrum. The obvious question of the relationship between these waves and the electrons remains. Elliott et al. (2018) have shown that whistler mode hiss that is strongly correlated with upgoing energetic electron beams over the polar cap at Jupiter (Tetrick et al., 2017) can explain at least part of the pitch angle scattering of the electrons; hence, we expect that some such scattering may occur for the precipitating electrons discussed here. While the inverted V electron spectrum is clearly due to a field aligned potential, the broadband electron spectrum requires some stochastic acceleration mechanism. We leave the question of possible electron acceleration by the observed plasma waves to a follow-on paper.

Acknowledgments
The research at the University of Iowa is supported by NASA through contract 699041X with the Southwest Research Institute. O.S. acknowledges support from the LTAUSA17070 grant and from the Praemium Academiae award. Data used in this paper are archived in the Planetary Data System (https://pds.nasa.gov/).

References

Amm, O., Birn, J., Bonnell, J., Borovsky, J. E., Carbary, J. F., Carlson, C. W., et al. (2002). Chapter 4—In situ measurements in the auroral plasma. *Space Science Reviews*, *103*(1/4), 93–208. https://doi.org/10.1023/A:1023082700768

Bolton, S. J., Lunine, J., Stevenson, D., Connerney, J. E. P., Levin, S., Owen, T. C., et al. (2017). *Space Science Reviews*, *213*(1-4), 5–37. https://doi.org/10.1007/s11214-017-0429-6

Bonfond, B., Grodent, D., Gérard, J.-C., Stallard, T., Clarke, J. T., Yoneda, M., & Radioti, & A., Gustin, J. (2012). Auroral evidence of Io's control over the magnetosphere of Jupiter. *Geophysical Research Letters*, *39*, L01105. https://doi.org/10.1029/2011GL050253

Carlson, C. W., Pfaff, R. F., & Watzin, J. G. (1998). The Fast Auroral SnapshoT (FAST) mission. *Geophysical Research Letters*, *25*(12), 2013–2016. https://doi.org/10.1029/98GL01592

Chaston, C. C., Carlson, C. W., Peria, W. J., Ergun, R. E., & McFadden, J. P. (1999). FAST observations of inertial Alfven waves in the dayside aurora. *Geophysical Research Letters*, *26*(6), 647–650. https://doi.org/10.1029/1998GL900246

Connerney, J. E. P., Benn, M., Bjarno, J. B., Denver, T., Espley, J., Jorgensen, P. S., et al. (2017). The Juno magnetic field investigation. *Space Science Reviews*, *213*(1-4), 39–138. https://doi.org/10.1007/s11214-017-0334-z

Connerney, J. E. P., Kotsiaros, S., Oliversen, R. J., Espley, J. R., Joergensen, J. L., Joergensen, P. S., et al. (2018). A new model of Jupiter's magnetic field from Juno's first nine orbits. *Geophysical Research Letters*, *45*, 2590–2596. https://doi.org/10.1002/2018GL077312

Elliott, S. S., Gurnett, D. A., Kurth, W. S., Clark, G., Mauk, B. H., Bolton, S. J., et al. (2018). Pitch angle scattering of upgoing electron beams in Jupiter's polar regions by whistler mode waves. *Geophysical Research Letters*, *45*, 1246–1252. https://doi.org/10.1002/2017GL076878

Kolmasova, I., Imai, M., Santolik, O., Kurth, W. S., Hospodarsky, G. B., Gurnett, D. A., et al. (2018). Discovery of rapid whistlers close to Jupiter implying similar lightning rates as on Earth. *Nature Astronomy*, *2*, 5, https://doi.org/10.1038/s41550-018-0442-z

Kurth, W. S., Hospodarsky, G. B., Kirchner, D. L., Mokryzcki, B. T., Averkamp, T. F., Robison, W. T., et al. (2017). The Juno waves investigation. *Space Science Reviews*, *213*(1-4), 347–392. https://doi.org/10.1007/s11214-017-0396-y

Mauk, B. H., Haggerty, D. K., Jaskulek, S. E., Schlemm, C. E., Brown, L. E., Cooper, S. A., et al. (2017a). The Jupiter Energetic Particle Detector Instrument (JEDI) investigation for the Juno mission. *Space Science Reviews*, *213*, 289–346. https://doi.org/10.1007/s11214-013-0025-3

Mauk, B. H., Haggerty, D. K., Paranicas, C., Clark, G., Kollmann, P., Rymer, A. M., et al. (2017b). Discrete and broadband electron acceleration in Jupiter's powerful aurora. *Nature*, *549*(7670), 66–69. https://doi.org/10.1038/nature23648

Mauk, B. H., Haggerty, D. K., Paranicas, C., Clark, G., Kollmann, P., Rymer, A. M., et al. (2018). Diverse electron and ion acceleration characteristics observed over Jupiter's main aurora. *Geophysical Research Letters*, *45*, 1277–1285. https://doi.org/10.1002/2017GL076901

Mosier, S. R., & Gurnett, D. A. (1971). Theory of the Injun 5 very-low-frequency Poynting flux measurements. *Journal of Geophysical Research*, *76*(4), 972–977. https://doi.org/10.1029/JA076i004p00972

Paschmann, G., Haaland, S., & Treumann, R. (2003). In situ measurements in the auroral plasma, chapter 4 in Auroral plasma physics. *Space Sciences Series of ISSI (International Space Sciences Institute)*, *15*, 93–208. AIP-press. https://doi.org/10.1007/978-94-007-1086-3

Strangeway, R. J., Kepko, L., Elphic, R. C., Carlson, C. W., Ergun, R. E., McFadden, J. P., et al. (1998). FAST observations of VLF waves in the auroral zone: Evidence of very low plasma densities. *Geophysical Research Letters*, *25*(12), 2065–2068. https://doi.org/10.1029/98GL00664

Tetrick, S. S., Gurnett, D. A., Kurth, W. S., Imai, M., Hospodarsky, G. B., Bolton, S. J., et al. (2017). Plasma waves in Jupiter's high latitude regions: Observations from the Juno spacecraft. *Geophysical Research Letters*, *44*, 4447–4454. https://doi.org/10.1002/2017GL073073